MATERIALS PHYSICS AND MECHANICS RESEARCH ARTICLE

Submitted: February 10, 2026 Revised: June 3, 2026 Accepted: July 2, 2026

Enhanced antibacterial performance of ZnO-Co_3O_4 nanocomposites for effective pathogenic bacteria control

M. Zahid [1], A. Rahim [1], M. Salim [2], M. Saleem [1], A. Ur Rahman [2], S. Zaheer Ud Din [3]✉

[1] Shandong Normal University, Jinan, P.R. China

[2] Hazara University Mansehra, Mansehra, Pakistan

[3] Hubei University of Automotive Technology, Shiyan, P.R. China

✉ zaheeruddin@yahoo.com

ABSTRACT

The rise of antibiotic resistance necessitates the development of advanced antibacterial agents. Here, a ZnO-Co_3O_4 nanocomposite with varying concentrations is synthesized via the sol-gel method. The structural and morphological features of the as-synthesized nanocomposite are characterized using X-ray diffraction, scanning electron microscopy, and Fourier-transform infrared spectroscopy techniques. The composite design enhances antibacterial performance compared to single oxides. The results revealed that ZnO-Co_3O_4 nanocomposites exhibit concentration-dependent morphology and antibacterial activity. Notably, ZnO-Co_3O_4 nanocomposites demonstrated superior antibacterial activity compared to pure ZnO. The addition of cobalt oxide decreased the size of the nanoparticles, thereby enhancing their antibacterial activity, particularly against Gram-positive bacteria, compared to Gram-negative bacteria. This enhanced activity is attributed to the increased production of reactive oxygen species and the improved penetration capability of the nanocomposite.

KEYWORDS

antibacterial activity • nanocomposites • sol-gel • reactive oxygen species

Citation: Zahid M, Rahim A, Salim M, Saleem M, Ur Rahman A, Zaheer Ud Din S. Enhanced antibacterial performance of ZnO-Co_3O_4 nanocomposites for effective pathogenic bacteria control. *Materials Physics and Mechanics*. 2026;54(4): 124–133.

http://dx.doi.org/10.18149/MPM.5442026_11

Introduction

The overuse of antibiotics has led to the emergence of antimicrobial resistance, which poses a significant danger to global human health. As a result of the emergence of treatment resistance in pathogenic microorganisms, formerly manageable diseases are increasingly becoming fatal [1]. Consequently, innovative techniques and methodologies are urgently required to address the significant healthcare problem presented by the fast growth of antibiotic-resistant microorganisms [2]. Antibacterial agents are classified into two primary categories: organic and inorganic [3]. The primary concern with traditionally employed organic antibacterial agents is their poor stability under elevated temperatures and pressures, whereas inorganic antibacterial agents exhibit superior stability and resilience [4].

Recent advancements in nanotechnology provide innovative methods for the creation of inorganic antibiotics with better effectiveness. Numerous studies have shown that inorganic functional nanomaterials, including Ag, TiO_2, MgO, CuO, and reduced graphene

© M. Zahid, A. Rahim, M. Salim, M. Saleem, A. Ur Rahman, S. Zaheer Ud Din, 2026.
Publisher: Peter the Great St. Petersburg Polytechnic University
This is an open access article under the CC BY-NC 4.0 license (https://creativecommons.org/li-censes/by-nc/4.0/)

oxide (RGO), can impede the development rate of multi-drug-resistant bacteria, including both Gram-positive and Gram-negative strains [5–9]. Among these nanomaterials, ZnO is distinguished by its inexpensive cost, great biocompatibility, and significantly enhanced antibacterial efficiency [10]. Moreover, ZnO is an extensively researched semiconductor characterized by a broad band gap energy of 3.37 eV and a high exciton binding energy of 60 meV [11–14]. Additionally, bacteria easily adhere to the surface of ZnO nanosheets. The nanoparticles then get inside the bacterial cells and damage the cell wall and membrane, which stops the bacteria from growing [15]. Moreover, ZnO demonstrated effectiveness against several bacterial strains, including both Gram-positive and Gram-negative bacteria, as documented by several research articles [16–19]. Their methodology involves disrupting bacterial cell membranes and generating ROS (reactive oxygen species) [20,21]. The generation of ROS, especially singlet oxygen and hydroxyl radicals, which are extremely reactive and aid in the oxidation of organic molecules as well as the utter destruction of bacteria and viruses, is the primary factor influencing the photodynamic antibacterial efficiency of ZnO nanostructures [22–24]. These ROS result from photogenerated electron-hole pairs that dissociate water molecules. Further, nanoscale ZnO enhances the formation of hydroxyl radicals due to its elevated surface area, leading to increased surface reactions [25–27]. Consequently, the antibacterial efficiency of ZnO nanostructures may be significantly improved by reducing the recombination rate of electron-hole pairs and activating them with visible light [28].

To overcome these drawbacks, combining ZnO with Cobalt oxide (Co_3O_4), which is a narrow-bandgap p-type semiconductor with antibacterial activity, can decrease the recombination rate of the carriers [29]. Although studies on Co_3O_4 nanoparticles are less extensive than those on ZnO, existing research demonstrates their effectiveness against infections such as Fusarium oxysporum, underscoring their potential for biological applications [30]. The combination of two metal oxides in a binary system can yield enhanced properties, such as superior thermal stability, higher electrical conductivity, and sensitive catalytic activity [31].

In this work, we presented the synthesis of ZnO and ZnO-Co_3O_4 nanocomposites with different concentrations through the Sol-Gel method. The structural, morphological, and optical characteristics of ZnO and Co_3O_4 nanocomposites were examined. Morphologically small nanoparticles with a high cobalt oxide concentration ratio possess high penetration power in the bacterial cells. This nanocomposite shows excellent antibacterial activity against Gram-positive bacteria compared to Gram-negative bacteria.

Materials and Methods

Zinc Nitrate hexahydrate $Zn(NO_3)_2 \cdot 6H_2O$ 98.0 % Cobalt Nitrate hexahydrate $Co(NO_3)_2$ 97 %, NaOH, Mueller-Hinton Agar, Staphylococcus aureus, Streptococcus pyogenes, Pseudomonas, Klebsiella, and distilled water were purchased from Shanghai Macklin Biochemical Co., Ltd. For the preparation of pure ZnO nanoparticles, the sol-gel method was used. 10.4 g of zinc nitrate hexahydrate was dissolved in 100 ml of deionized (DI) water and stirred for 15 min to obtain a homogeneous colorless solution. The zinc nitrate solution was kept on a hot plate, and the sodium hydroxide solution (4 g + 100 ml of DI) was added dropwise. During stirring, the zinc nitrate solution gradually changed to

a white gel. The gel was washed three times with DI water. The white gel was dried in an air oven at 120 °C. The synthesized samples were calcinated at 350 °C for 3.5 h to remove the moisture and improve the crystallinity.

The zinc oxide- cobalt oxide nanocomposites were obtained by dissolving 13.4 g of zinc nitrate hexahydrate into 100 ml of DI water and stirring for 15 min. Further, 1.5 g of cobalt nitrate hexahydrate dissolved in 100 ml of DI water and stirred for 15 min resulted in a pink solution, followed by mixing of both solutions via a magnetic hot plate. The NaOH solution was then added dropwise into the mixed solution. The gel was washed three times with DI water and dried at 120 °C in an air oven. Next, the dried nanocomposites were calcinated at 350 °C for 3.5 h, changing color from white to grey. The same procedure was used for ZnO-Co_3O_4 (20 %) and ZnO-Co_3O_4 (40 %) with different concentrations of zinc nitrate hexahydrate and cobalt nitrate hexahydrate.

5 g of Mueller-Hinton Agar was dissolved in 130 ml of distilled water for use as the test medium. The medium was sterilized in an autoclave for 15 min at 120 °C. The sterilized medium was poured into a sterile Petri dish, followed by freezing in the freezer. Five wells were made in sterile Petri dishes for checking bacterial zone inhibition, one for control and four for as-prepared samples. A 40 ml of bacterial suspension was applied to each Petri dish using soft cotton until it was evenly dispersed. A volume of 70 ml of DI water and the as-synthesized nanocomposites at varying concentrations were added to five separate wells. The Petri dish was incubated overnight at 37 °C.

Cobalt oxide Co_3O_4 produces ROS through many mechanisms, making it important in catalysis, ecological remediation, and biomedical applications. Oxygen vacancies on the Co_3O_4 superficial localized electrons, smoothing the activation of molecular oxygen (O_2) into superoxide anions ($O_2^{\bullet-}$) and other ROS, enhancing its catalytic activity [32]. Moreover, Co_3O_4 nanoparticles interact with hydrogen peroxide (H_2O_2), forming hydroxyl radicals (OH^-), which contribute to oxidative stress. The spin states of cobalt ions at Co_3O_4 interfaces more strongly influence their ability to activate molecules like O_2, affecting ROS generation. In the oxygen evolution reaction (OER), Co_3O_4 acts as a catalyst, facilitating the creation of ROS mediators like superoxide species [33]. Furthermore, its high surface reducibility enables continuous oxygen and water activation, ensuring continued ROS production for applications like contaminant degradation. These properties make Co_3O_4 a highly operative material for several oxidative processes [34]. ZnO-Co_3O_4 exhibits photocatalytic properties under light treatment, producing electron-hole pairs (e^-/h^+) contributing to ROS creation. The conduction band electrons decrease oxygen (O_2) to form superoxide anions ($O_2^{\bullet-}$). The valence band holes oxidize water molecules (H_2O) to produce hydroxyl radicals (OH^-) [15].

Figure 1 shows a schematic diagram presenting the synthesis of the ZnO-Co_3O_4 nanocomposite. The process begins with preparing individual zinc nitrate and cobalt nitrate solutions, which are mixed and stirred until homogeneous, followed by centrifugation. The precipitate is dried in an oven to eliminate residual solvent and calcined at high temperatures to form a crystalline ZnO-Co_3O_4 nanocomposite structure. The synthesized materials were analyzed using a Fourier transform infrared (FTIR) spectrometer (Perkin-Elmer Spectrum 100 Series), a scanning electron microscope (Jeol JSM-6510 LV), and X-ray diffraction (Bruker AXS D8 FOCUS Diffractometer) with Cu Kα (λ = 1.54056 Å) radiation.

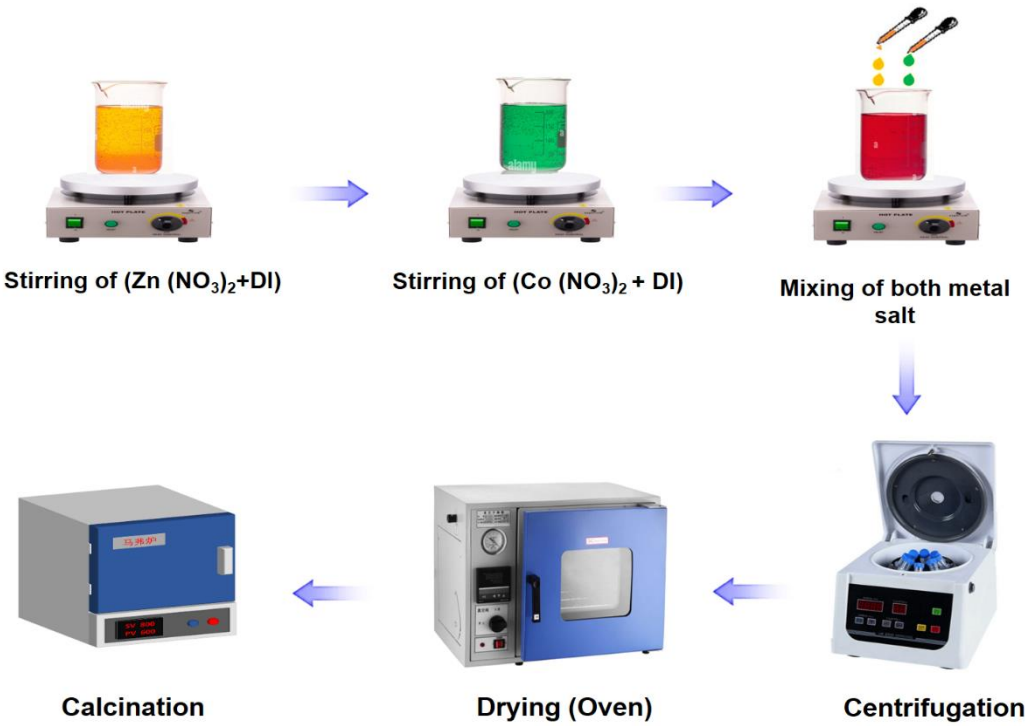


Fig. 1. Synthesis of ZnO and ZnO-Co_3O_4 nanocomposites

Results and Discussion

X-ray diffraction analysis

The crystallinity was confirmed through XRD (X-ray diffraction) spectra (2θ: 30–80°) of pure ZnO and ZnO-Co_3O_4 nanocomposites, shown in Fig. 2(a), with all peaks corresponding to ZnO (01-080-0075). The diffraction peaks for pure ZnO are observed at 31.47, 34.4, 36.3, 47.5, 56.5, 62.9, 67.9, and 76.8°, corresponding to the (100), (101), (002), (102), (110), (200), (103), and (102) planes, respectively. The average crystalline size was calculated using the Debye-Scherrer formula [35]:

$$D = K\frac{\lambda}{B}cos\theta, \quad (1)$$

where D denotes a crystallite size, K represents the Scherrer constant, λ stands for the X-ray wavelength, and B is the full width at half maximum in radians [36]. The crystalline sizes (average) for pure ZnO and ZnO-Co_3O_4 nanocomposites (10, 20, 40 %) are 51.5, 46.5, 41.5, and 36.3 nm, respectively. ZnO exhibits a hexagonal lattice structure with parameters $a = b = 3.25$ Å and $c = 5.3$ Å. No peaks were observed from cobalt oxide, confirming that the pure and well-crystallized ZnO was consistent with the literature [36].

Figure 2(b) illustrates the FT-IR (Fourier-transform infrared spectroscopy) spectrum of ZnO-Co_3O_4 (10, 20, and 40 %) nanocomposites. The 3791 and 1340 cm^{-1} absorption spectra correspond to O-H stretching vibrations from water molecules during fabrication [37]. The peak at 831 cm^{-1} corresponds to Co-O stretching within the tetrahedral coordination of Co^{2+}, while the peak at 653 cm^{-1} is related to Co-O stretching in the octahedral coordination of Co^{3+}. The Zn-O stretching vibration is seen at 553 cm^{-1}, influenced by the presence of cobalt oxide. The appearance of Zn-O and Co-O peaks confirms the successful synthesis of ZnO-Co_3O_4 nanocomposites [38].

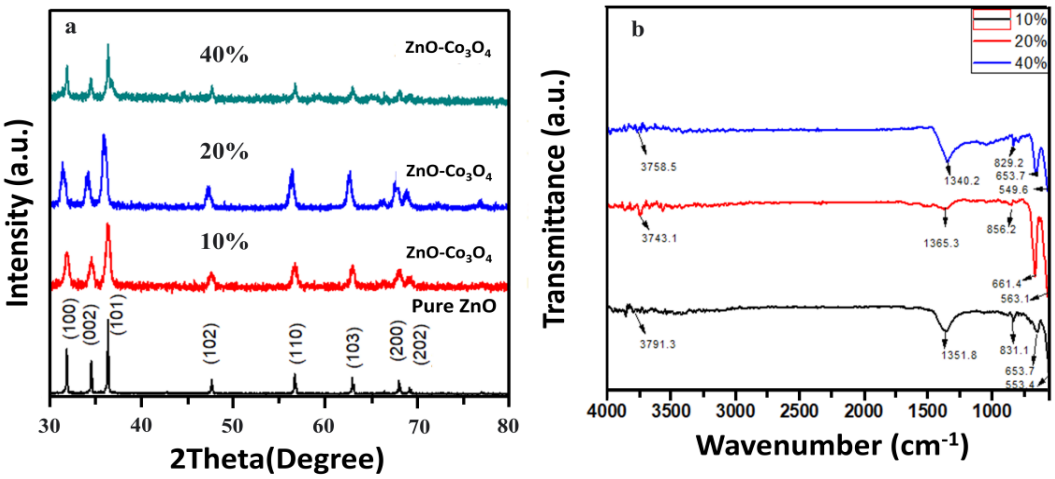


Fig. 2. (a) X-ray diffraction patterns of pure ZnO and ZnO-Co_3O_4 nanocomposites and (b) FT-IR spectra of ZnO-Co_3O_4 with 10, 20, and 40 % compositions

Morphological and elemental composition

The morphological study of pure ZnO and ZnO-Co_3O_4 nanocomposites was carried out through scanning electron microscopy (SEM). The SEM images (Fig. 3) show that pure ZnO and its nanocomposites with 10, 20, and 40 % cobalt oxide concentrations exhibit

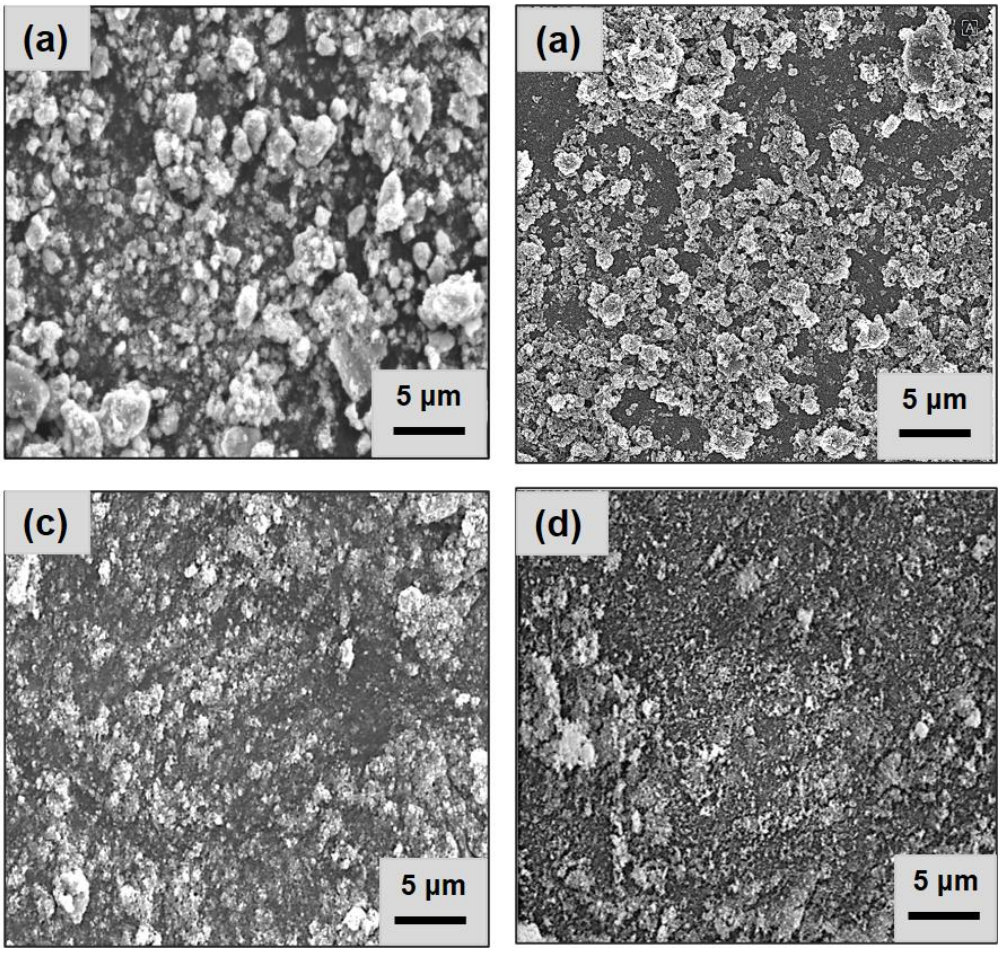


Fig. 3. SEM micrographs of pure ZnO and ZnO-Co_3O_4 nanocomposites at different concentrations: (a) pure ZnO, (b) ZnO-Co_3O_4 (10 %), (c) ZnO-Co_3O_4 (20%), and (d) ZnO-Co_3O_4 (40 %)

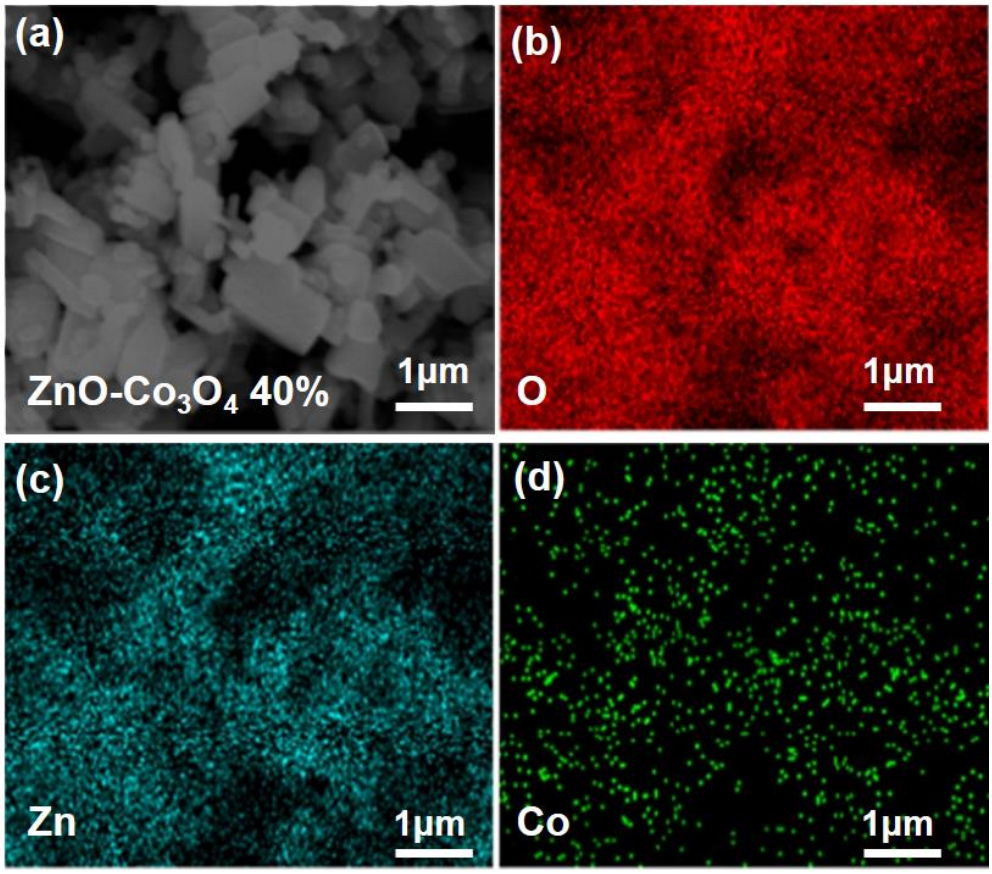


Fig. 4. EDS and elemental mapping of ZnO-Co_3O_4 nanocomposite showing (a) EDS spectrum, (b) oxygen (O) distribution, (c) zinc (Zn) distribution, and (d) cobalt (Co) distribution

varying morphologies and decreased an average crystallite size. The energy-dispersive X-ray spectroscopy (EDS) analysis (Fig. 4) confirms the successful synthesis of ZnO-Co_3O_4 with a 40 % composition. The elemental distributions of oxygen, zinc, and cobalt are illustrated in Fig. 4(b–d), respectively. The EDS mapping further verifies the uniform distribution of these elements, indicating the formation of ZnO-Co_3O_4 nanocomposites without any detectable impurities.

Antibacterial activities

This study examined the antibacterial properties of ZnO and ZnO-Co_3O_4 nanocomposites at varying concentrations. Nanocomposites with different ZnO-Co_3O_4 ratios were synthesized and evaluated against common bacterial strains to assess their effectiveness. Four plates were prepared, each containing five wells: a central well as the control without nanoparticles and four surrounding wells labeled Z pure ZnO, S1 (10 %) nanocomposites, (S2) 20 % nanocomposites, and S3 (40 %) nanocomposites, as shown in Fig. 5, This setup allowed precise monitoring of antibacterial effects, of pure ZnO nanoparticles showing zones of inhibition (ZOI) of 11 and 12.5 mm against the Gram-positive bacteria (*Streptococcus* and *Staphylococcus*) as shown in Fig. 5(a,b), respectively. While ZOIs against the Gram-negative bacteria (*Klebsiella pneumoniae* and *Pseudomonas*) are 8 mm for both bacterial strains, as shown in Fig. 5(c,d). Treatment with ZnO-Co_3O_4 with 40 % (labeled as S3) resulted in larger ZOIs (due to small size with high penetrating

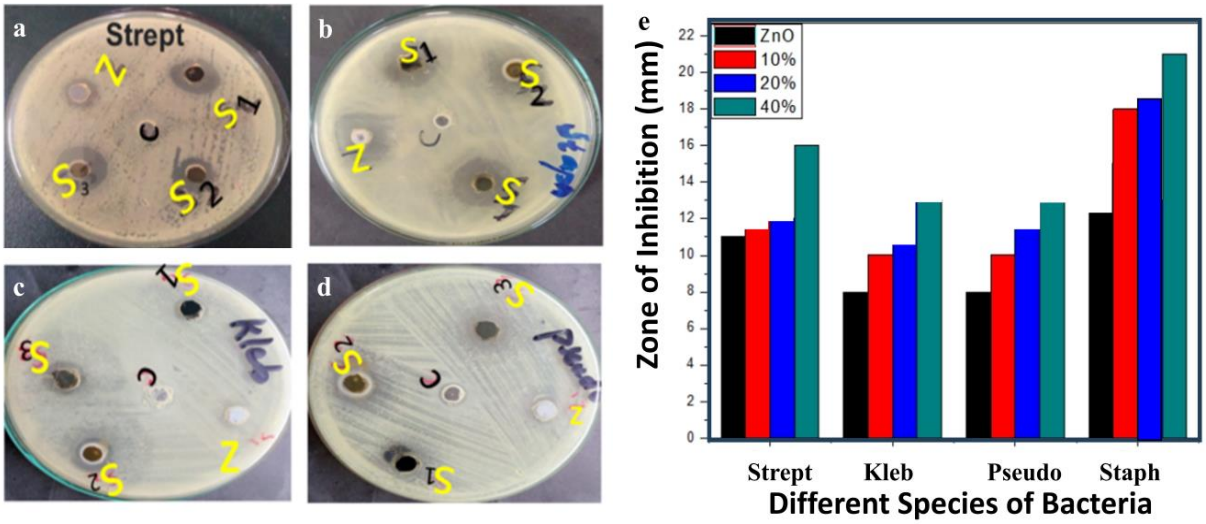


Fig. 5. Antibacterial activities of pure ZnO and ZnO-Co_3O_4 nanocomposites against different bacterial strains: (a) *S. streptococcus*, (b) *S. aureus*, (c) *Klebsiella*, (d) *Pseudomonas*, and (e) corresponding bar graph of zone of inhibition

power in the bacterial cell) for Gram-positive bacteria, with *Streptococcus* and *Staphylococcus*, showing ZOIs of 16 and 21.5 mm. In contrast, Gram-negative bacteria, *Pseudomonas* and *Klebsiella pneumoniae*, exhibited ZOIs of 13 mm each, as displayed in Fig. 5(a–d). Compared to ZnO-Co_3O_4 with 40%, the remaining ZnO-Co_3O_4 with 20% and 10 % present a lower performance ZOI against bacteria, as shown in Fig. 5(a–d).

These findings demonstrate the sensitivity of Gram-positive bacteria to ZnO nanoparticles and their resulting composites, especially *Staphylococcus* aureus bacteria. Pure ZnO-NPs with a concentration of 70 µg/mL reduced the growth of *Streptococcus* (Gram +ve) to a larger extent than *Klebsiella* (Gram -ve). However, their composites at different sizes posed a greater resistance to the growth of *Streptococcus* (Gram +ve) than *Klebsiella* (Gram -ve). Exposure of the bacterial species to different sizes of the composite particles resulted in a higher reduction in the growth of *Staphylococcus* (Gram +ve) compared to *Pseudomonas* species (Gram -ve). According to our results, the Gram +ve bacteria are more sensitive to ZnO nanocomposite with higher cobalt concentrations than lower and pure ZnO according to ZOIs, as shown in Table 1. Our results are better than the previously reported research on Cu-doped ZnO nanoparticles and different nanocomposites [39]. This antibacterial activity arises from ROS production in metallic oxide nanocomposites, which in turn causes DNA damage and, eventually, cell death. ZnO nanoparticles and their composites showed antimicrobial potential against the pathogens, indicating that they can be used in the pharmaceutical industry to cure diseases caused by bacteria due to their safe status and low cost.

Table 1. Average zone of inhibition of ZnO and ZnO-Co_3O_4 nanocomposites

	Bacteria	**Concentrations**		**ZnO**	**ZnO-Co_3O_4**		
					10%	20%	40%
Gram +ve	*Streptococcus*	70 µg/mL	Zone of inhibition (mm)	11	14	12	16
	Staphylococcus	70 µg/mL		12.5	18	19	21.5
Gram -ve	*Klebsiella*	70 µg/mL		8	10	14	13
	Pseudomonas	70 µg/mL		8	10	14	13

Conclusion

In summary, pure ZnO and ZnO-Co_3O_4 nanocomposites with varying concentrations (10, 20, 40 %) were synthesized using the sol-gel method and evaluated for their antibacterial activity against four bacterial strains, including both Gram-positive and Gram-negative bacteria. 40 % nanocomposites showed higher zone inhibition against the Gram-positive bacteria due to the small size and high ROS compared to the 10 and 20 %, respectively. Our results indicate that Gram-positive bacteria are more sensitive compared to Gram-negative bacteria. This approach suggests a good approach to synthesizing a nanocomposite in an easy and cost-effective method for better antibacterial activity.

CRediT authorship contribution statement

Muhammad Zahid: writing – review & editing, writing – original draft, investigation, data curation; **Abdur Rahim**: writing – review & editing; **Muhammad Salim**: writing – review & editing; **Muhammad Saleem**: writing – review & editing; **Atta Ur Rahman**: writing – review & editing; **Syed Zaheer Ud Din**: writing – review & editing, conceptualization, supervision.

Conflict of interest

The authors declare that they have no conflict of interest.

References

1. Farrukh M, Munawar A, Nawaz Z, Hussain N, Hafeez AB, Szweda P. Antibiotic resistance and preventive strategies in foodborne pathogenic bacteria: A comprehensive review. *Food Science and Biotechnology.* 2025;34(10): 2101–2129.
2. Nwobodo DC, Ugwu MC, Anie CO, Al-Ouqaili MTS, Ikem JC, Chigozie UV, Saki M. Antibiotic resistance: The challenges and some emerging strategies for tackling a global menace. *Journal of Clinical Laboratory Analysis.* 2022;36(9): e24655.
3. Saidin S, Jumat MA, Amin NAAM, Al-Hammadi ASS. Organic and inorganic antibacterial approaches in combating bacterial infection for biomedical application. *Materials Science and Engineering: C.* 2021;118: 111382.
4. Raza S, Matuła K, Karoń S, Paczesny J. Resistance and adaptation of bacteria to non-antibiotic antibacterial agents: Physical stressors, nanoparticles, and bacteriophages. *Antibiotics.* 2021;10(4): 435.
5. Saravanan H, Subramani T, Rajaramon S, David H, Sajeevan A, Sujith S, Solomon AP. Exploring nanocomposites for controlling infectious microorganisms: Charting the path forward in antimicrobial strategies. *Frontiers in Pharmacology.* 2023;14: 1282073.
6. Pardhi DM, Karaman DŞ, Timonen J, Wu W, Zhang Q, Satija S, Mehta M, Charbe N, McCarron PA, Tambuwala MM, Bakshi HA, Negi P, Aljabali AA, Dua K, Chellappan DK, Behera A, Pathak K, Watharkar RB, Rautio J, Rosenholm JM. Anti-bacterial activity of inorganic nanomaterials and their antimicrobial peptide conjugates against resistant and non-resistant pathogens. *International Journal of Pharmaceutics.* 2020;586: 119531.
7. Mubeen B, Ansar AN, Rasool R, Ullah I, Imam SS, Alshehri S, Ghoneim MM, Alzarea SI, Nadeem MS, Kazmi I. Nanotechnology as a novel approach in combating microbes providing an alternative to antibiotics. *Antibiotics.* 2021;10(12): 1473.
8. Zemtsova EG, Smirnov VM, Kozlova LA, Morozov PE, Yurchuk DV, Semenov BN, Morozov NF. Development of aluminum-based composite with two reinforcing modifiers (TiC/Ni, CNTs/Ni) with improved mechanical properties. *Materials Physics and Mechanics.* 2023;51(3): 9–19.
9. Kumar N, Singh D, Nigam A, Rajpoot O, Yadav MK, Singh YP, Prakash PS, Singh S. Structural and magnetic properties of zinc doped copper ferrite synthesized by sol-gel and hydrothermal route. *Materials Physics and Mechanics.* 2021;47(2): 306–314.

10. Kumar R, Umar A, Kumar G, Nalwa HS. Antimicrobial properties of ZnO nanomaterials: A review. *Ceramics International.* 2017;43(5): 3940-3961.
11. Ungula J. *Growth and characterization of ZnO nanoparticles by sol-gel process. PhD thesis*. University of the Free State (Qwaqwa Campus); 2015.
12. Samadi M, Zirak M, Naseri A, Khorashadizade E, Moshfegh AZ. Recent progress on doped ZnO nanostructures for visible-light photocatalysis. *Thin Solid Films.* 2016;605: 2–19.
13. Ungula J, Dejene B. Effect of solvent medium on the structural, morphological and optical properties of ZnO nanoparticles synthesized by the sol–gel method. *Physica B: Condensed Matter.* 2016;480: 26–30.
14. Van Tuyen N, Kolesnikova AL, MYu G, Romanov AE. Band gap engineering with strains induced by quantum dots in semiconductors nanowires. *Materials Physics and Mechanics.* 2025;53(5): 42–49.
15. Ali Z, Mehboob S, Farooq M, Khan M, Fareed I, Fatima Z, Yunas MF. Synthesis of ZnO-Co_3O_4 Nanocomposites for Efficient Methylene Blue Degradation under Solar Light Irradiation. *Russian Journal of Physical Chemistry A.* 2024;98(7): 1592–1606.
16. Azam A, Ahmed AS, Oves M, Khan MS, Habib SS, Memic A. Antimicrobial activity of metal oxide nanoparticles against Gram-positive and Gram-negative bacteria: a comparative study. *International Journal of Nanomedicine.* 2012;(7): 6003–6009.
17. Hoseinzadeh E, Alikhani MY, Samarghandi M-R, Shirzad-Siboni M. Antimicrobial potential of synthesized zinc oxide nanoparticles against gram positive and gram negative bacteria. *Desalination and Water Treatment.* 2014;52(25–27): 4969–4976.
18. Yusof NAA, Zain NM, Pauzi N. Synthesis of ZnO nanoparticles with chitosan as stabilizing agent and their antibacterial properties against Gram-positive and Gram-negative bacteria. *International Journal of Biological Macromolecules.* 2019;124: 1132–1136.
19. Babayevska N, Przysiecka Ł, Iatsunskyi I, Nowaczyk G, Jarek M, Janiszewska E, and Jurga S. ZnO size and shape effect on antibacterial activity and cytotoxicity profile. *Scientific Reports.* 2022;12: 8148–8161.
20. Su HL, Chou CC, Hung DJ, Lin SH, Pao IC, Lin JH, Huang FL, Dong RX. The disruption of bacterial membrane integrity through ROS generation induced by nanohybrids of silver and clay. *Biomaterials.* 2009;30(30): 5979–5987.
21. Dharmaraja AT. Role of reactive oxygen species (ROS) in therapeutics and drug resistance in cancer and bacteria. *Journal of Medicinal Chemistry.* 2017;60(8): 3221–3240.
22. Maeda H, Akaike T. Oxygen free radicals as pathogenic molecules in viral diseases. *Proceedings of the Society for Experimental Biology and Medicine.* 1991;198(2): 721–727.
23. Imlay JA. The molecular mechanisms and physiological consequences of oxidative stress: lessons from a model bacterium. *Nature Reviews Microbiology.* 2013;11(7): 443–454.
24. Samran B, Timah EN, Phatungthane T, Thongpanit P, Kadroon B, Photharin S, Chaiwichian S. Fabrication and characterization of zinc nitrate doped TiO_2 nanotubes for dye-sensitized solar cells. *Materials Physics and Mechanics.* 2025;53(5): 83–89.
25. Raha S, Ahmaruzzaman M. ZnO nanostructured materials and their potential applications: progress, challenges and perspectives. *Nanoscale Advances.* 2022;4(8): 1868–1925.
26. Xin H, Liu Y, Xiao Y, Wen M, Sheng L, Jia Z. Design and Nanoengineering of Photoactive Antimicrobials for Bioapplications: from Fundamentals to Advanced Strategies. *Advanced Functional Materials.* 2024;(34(38): 2402607.
27. Kukushkin SA, Osipov AV, Kasatkin IA, Mikhailovskii VY, Romanychev AI. Formation of ordered ZnO structures grown by the ALD method on hybrid SiC/Si (100) substrates. *Materials Physics and Mechanics.* 2019;42(1): 30–39.
28. Qi K, Cheng B, Yu J, Ho W. Review on the improvement of the photocatalytic and antibacterial activities of ZnO. *Journal of Alloys and Compounds.* 2017;727: 792–820.
29. Abdullah M, Akhtar MS, Al-Abbas SM. Facile growth and promising applications of cobalt oxide (Co_3O_4) nanoparticles as chemi-sensor and dielectric material. *Current Nanoscience.* 2018;14(4): 343–351.
30. Velmurugan S, Yang TCK, Chen SW, Chen JN. Metal-organic frameworks derived ZnO-Co_3O_4 pn heterojunction photocatalyst for the photoelectrochemical detection of sulfadiazine. *Journal of Environmental Chemical Engineering.* 2021;9(5): 106169.
31. Shaheen N, Aadil M, Zulfiqar S, Sabeeh H, Agboola PO, Warsi MF, Aly Aboud MF, Shakir I. Fabrication of different conductive matrix supported binary metal oxides for supercapacitors applications. *Ceramics International.* 2021;47(4): 5273–5285.

32. Liu Y, Peng Y, Naschitzki M, Gewinner S, Schöllkopf W, Kuhlenbeck H, Pentcheva R, Cuenya BR. Surface oxygen vacancies on reduced Co_3O_4 (100): superoxide formation and ultra-low-temperature CO oxidation. *Angewandte Chemie International Edition.* 2021;60(30): 16514–16520.
33. Bayati-Komitaki N, Ganduh SH, Alzaidy AH, Salavati-Niasari M. A comprehensive review of Co_3O_4 nanostructures in cancer: Synthesis, characterization, reactive oxygen species mechanisms, and therapeutic applications. *Biomedicine & Pharmacotherapy.* 2024;180: 117457.
34. Lei J, Zhang L, Li M, Liu W, Jin Y, Li B. Surface Oxygen Vacancy-Rich Co_3O_4 Nanowires as an Effective Catalyst of Luminol–H2O2 Chemiluminescence for Sensitive Immunoassay. *RSC Advances.* 2023;95(48): 17937–17944.
35. Li J, Sathasivam S, Taylor A, Carmalt CJ, Parkin IP. Single step route to highly transparent, conductive and hazy aluminium doped zinc oxide films. *RSC Advances.* 2018;8(74): 42300–42307.
36. Holzwarth U, Gibson N. The Scherrer equation versus the'Debye-Scherrer equation'. *Nature Nanotechnology.* 2011;6(9): 534.
37. Mekuye B, Abera B. Nanomaterials: An overview of synthesis, classification, characterization, and applications. *Nano Select.* 2023;4(8): 486–501.
38. Jiang H, Liu S, Liang L, Lu W. Oxygen plasma assisted enhanced photoresponse of ZnO nanowires fabricated by catalyst-free chemical vapor deposition. *RSC Advances.* 2018;8(51): 28928–28933.
39. Raju P, Deivatamil D, Martin Mark JA, Jesuraj JP. Antibacterial and catalytic activity of Cu doped ZnO nanoparticles: structural, optical, and morphological study. *Journal of the Iranian Chemical Society.* 2022;19(3): 861–872.